2024 IEEE International Conference on Robotics and Automation (ICRA 2024)
May 13-17, 2024. Yokohama, Japan

A Novel Fish-inspired Self-adaptive Approach to Collective Escape of Swarm Robots Based on Neurodynamic Models

Junfei Li, *Member, IEEE* and Simon X. Yang, *Senior Member, IEEE*

***Abstract*— Fish schools present high-efficiency group behaviors to collective migration and dynamic escape from the predator through simple individual interactions. The purpose of this research is to infuse swarm robots with "fish-like" intelligence that will enable safe navigation and efficient cooperation, and successful completion of escape tasks in changing environments. In this paper, a novel fish-inspired self-adaptive approach is proposed for the collective escape of swarm robots. A bio-inspired neural network (BINN) is introduced to generate collision-free escape trajectories through the dynamics of neural activity and the combination of attractive and repulsive forces. In addition, a neurodynamics-based self-adaptive mechanism is proposed to improve the self-adaptive performance of the swarm robots in dynamic environments. Similar to fish escape maneuvers, simulations and real-robot experiments show that the swarm robots can collectively leave away from the threat and respond to sudden environmental changes. Several comparison studies demonstrated that the proposed approach can significantly improve the effectiveness, efficiency, and flexibility of swarm robots in complex environments.**

I. Introduction

Recently, many types of research have involved exploiting the understanding of mechanisms to achieve the collective behaviors of swarm robots [1]–[3]. Fish are known to have abilities to navigate and respond effectively to dynamic environments through the use of simple mechanisms [4]. Through cooperation and limited implicit communication, fish schools are able to accomplish complex tasks that would be beyond the capabilities of an individual fish [5]. The collective behavior of fish schools is achieved through visual mediates and the mechanosensory functions of the lateral line system [6]. The lateral line system facilitates the detection of water movements, therefore the fish adjusts the repulsion when individuals are too close, and allows fish to respond to rapid changes in the environment [7]. In the fields of robotics, methods about how to achieve collective escape behaviors are currently an active focus of research [8]–[11].

A solution to the distributed control architecture of robots is based on the fountain maneuver model [12]. Cioarga *et al.* [13] implemented collision-free fountain maneuvers for the mobile robots. Berlinger *et al.* [14] used the fountain maneuver model to design the underwater robotic platform that is able to leave a moving predator. Some research is also based on the artificial virtual forces, which are generated from nearby neighbors based on relative distance to achieve the collective behaviors of swarm robots. Berlinger *et al.* [15] used a potential field-based model to mimic collective behaviors for underwater robots in 3D environments. Connor *et al.* [16] proposed a fish-inspired robotic algorithm to mimic the collective behavior of avoiding predators. Novák *et al.* [17] proposed an animal-inspired fast escape method that allows swarm robots to avoid dynamic obstacles. Min and Wang [18] proposed a fish-inspired emergency mode transfer framework to escape the predator and avoid collision with obstacles. After that, Nogami and Wang [19] used the emergency mode transfer framework to the group emergency stop for the multi-mobile robot system. However, most fish-inspired robotic studies only considered the collision-free or static obstacle environment, which is not similar to the actual fish schools that can respond in real-time to rapidly changing environments. In addition, many studies required that the robot have full knowledge about the environment which is also not similar to the actual fish schools that are based on the limited implicit communication.

The purpose of this paper is to enable swarm robots with some desirable properties of fish escape behaviors. The swarm robots are considered as a group of simple robots that are autonomous and only have limited neighbor information. It is important to note the proposed collective escape is fish-inspired, but the core operation departs from the real fish through the introduction of the neurodynamics model. In real-world fish schools, the individual fish can detect the water movement to perceive neighbors through their lateral lines [6]. In this paper, the neurodynamics model is incorporated to improve self-adaptive performance in dynamic environments. In addition, a bio-inspired neural network (BINN) is introduced to generate collision-free escape trajectories and virtual forces. Simulation and experimental results have demonstrated the effectiveness of the proposed approach for ensuring safe escape and efficient self-adaptive cooperation among autonomous robots in changing environments. The main contributions of this paper are summarized as follows:

- A novel collective escape is proposed to swarm robots in changing environments. The proposed approach is inspired by the group escape behavior of fish.
- A novel collision-free virtual forces approach is proposed to guide swarm robots based on the BINN. During the escape process, there are no learning procedures for the movement of robots.
- A novel neurodynamics-based self-adaptive mechanism is proposed to consider the effects of obstacles, which enables swarm robots to dynamically adjust their pa-

This work was supported by Natural Sciences and Engineering Research Council (NSERC) of Canada.

Junfei Li and Simon X. Yang are with the Advanced Robotics and Intelligent Systems Laboratory, School of Engineering, University of Guelph, Guelph, ON N1G2W1, Canada. Emails: {jli64;syang}@uoguelph.ca

rameters in complex environments.

This paper is organized in the following manner. Section II gives the problem statement. Section III describes the proposed approaches. Section IV shows the simulation and comparison results. Section V provides a real robot experiment. In Section VI, the result is briefly summarized.

II. Problem Statement

For a swarm of m robots, their time-varying location at time instant t in the 2D Cartesian workspace W, can be uniquely determined by the spatial position $\mathbf{p}_e = (x_e, y_e)$, $e = 1, \ldots, m$. The maximum speed of the eth robot is denoted by $V_{max} > 0$. Suppose each robot is considered as an omnidirectional robot, which can change the moving direction without delay. The next location of the eth robot at time instant $t+1$ can be given as

$$(x_e)_{t+1} = (x_e)_t + v_k \Delta t \cos(\theta_e)_t \tag{1}$$

$$(y_e)_{t+1} = (y_e)_t + v_k \Delta t \sin(\theta_e)_t \tag{2}$$

where the $v_k < V_{max}$ is the current speed of the robot; θ_e is the moving direction of the robot; and Δt is the unit time interval. The robot is equipped with sensors with 360° visual capability and a detection range of R_s to recognize the threat and other robots. In addition, there is a sequence of static and moving obstacles in W. The collision-free area pertaining to static $\mathcal{O}$ can be defined as $\mathcal{O}_{\text{free}} := \{(x, y) \in \mathbb{R}^2 : \Gamma > 1\}$, where $\Gamma = (x - x_o)^2 + (y - y_o)^2 / \lambda_o$. The variable (x_o, y_o) is the center of the obstacle, and λ_o is the size of the obstacle. The regions meeting $\Gamma = 1$, $\Gamma > 1$, or $\Gamma < 1$ denote the surface, exterior, or interior of the obstacle, respectively. If moving obstacle scenarios exist, its time-varying collision-free area is defined as $\mathcal{O}^t_{\text{free}} := \{(x, y) \in \mathbb{R}^2 : \Gamma_t > 1\}$,where Γ_t has the same structure of Γ. The center of the moving obstacle (x^t_o, y^t_o) is updated with respect to a constant moving speed v_o. To be applicable in real-world scenarios, the escape of a swarm of robots must be able to meet the following requirements.

1) The robots cannot share threat information with each other, only the first robot to detect the threat is aware of its position.
2) The escape process must be self-adaptive to changing environments.
3) The robots must maintain the desired distance R_d from their neighbors during the escape process.

Therefore, the fish-inspired escape studied in this paper can be described as: for a group of m robots and given the initial positions of robots $\mathbf{p}_e(0)$ with $e = 1, \ldots, m$. Since the i-th robot detects a threat, the i-th robot begins to escape and generate a collision-free trajectory, that is, $\mathbf{P}_{\text{Escape}} \in \mathcal{O}_{\text{free}}$, until achieving a safe distance d_s. Other robots generated collision-free trajectories, that is, $\mathbf{P}_{\text{Follow}} \in \mathcal{O}_{\text{free}}$, to follow the i-th robot with the desired distance R_d to neighboring robots. During the escape process, the swarm robots are required to be self-adaptive to adapt to changing environments.

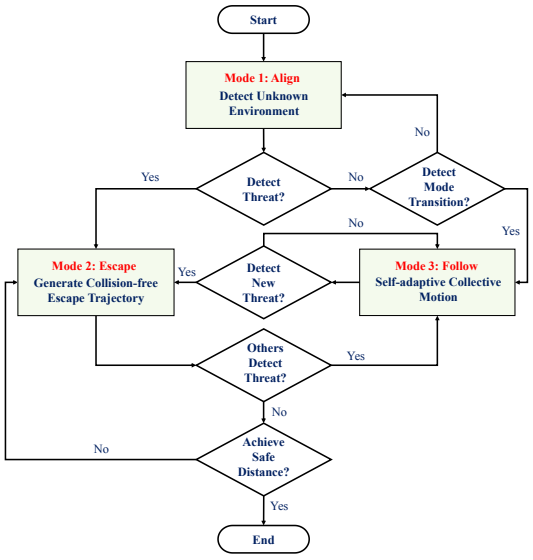

Fig. 1: The diagram of the mode transitions.

III. Proposed Approach

A. Fish-inspired Behavioral Modeling and Organization

Fish schools exhibit highly efficient group behaviors through simple individual interactions. In this paper, the escape behavior is modeled as a mode transition process. Each robot has three modes: *Align* mode, *Escape* mode, and *Follow* mode. The behavior of the robot is determined by a current mode. As shown in Fig. 1, the swarm robots start in the *Align* mode. In the case that the robot has not detected a threat within the sensor range R_s and any mode transitions from neighboring robots, the robot stays in *Align* mode. If the robot detects the threat, its *Align* mode transitions into the *Escape* mode. In the case that the robot detects that any neighboring robots transition into the *Escape* or *Follow* mode, this robot transitions into the *Follow* mode. In the case that the *Follow* robot detects a new threat, this robot transitions into the *Escape* mode, whereas the original *Escape* robot transitions into the *Follow* mode. In the event that the *Escape* robot achieves the safe distance d_s, the escape task is finished.

In addition, the fish organization was considered an egalitarian organization. Therefore, the traditional fish-inspired approaches assumed that swarm robots are an egalitarian organization [15]. However, the most current studies found that the hierarchical organization might exist in some species of fishes [4]. Therefore, inspired by Nagy *et al.* [20], a hierarchical organization is incorporated into the swarm robots. Once a robot detects the threat, the escape of this robot begins. At this time, a hierarchical index system is built to organize the swarm robots. The hierarchical index of the *Escape* robot is 1. The hierarchical index of robots within the detection range of the *Escape* robot is 2. For robots outside the detection range of the *Escape* robot, the hierarchical index is equal to the lowest hierarchical index of its neighbors add 1. The hierarchical organization can assist

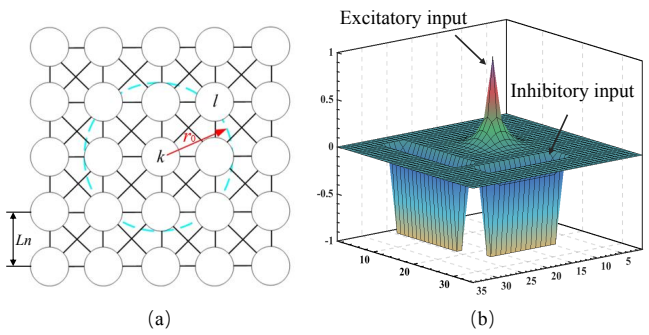

Fig. 2: Examples of the bio-inspired neural network. (a) structure of the neural network; (b) the dynamic landscape of neural activity.

Follow robots in generating the most appropriate attraction forces, thereby preventing robots from being drawn to other robots simultaneously.

B. Virtual Forces Based on Bio-inspired Neural Network

In this paper, a BINN is proposed to generate attractive and repulsive forces. The structure of the BINN is shown in Fig. 2(a). Each neuron is one-to-one representing an environmental location. Note that the distance between neurons L_n is assumed to equal to λ_o, which can guarantee the neuron one-to-one representing the size of the obstacle. Therefore, the receptive field of the neuron is represented by a circle with a radius of r_0 and has lateral connections only to its eight neighboring neurons. The shunting model was developed by Grossberg based on Hodgkin and Huxley's model [21]. The neural activity for the k-th neuron is written as

$$\begin{aligned}\frac{dx_k}{dt} = -Ax_k + (B - x_k)\left([I_k]^+ + \sum_{l=1}^{n} w_{kl}[x_l]^+\right) \\ - (D + x_k)\left([I_k]^- + \sum_{l=1}^{n} v_{kl}[x_l - \sigma]^-\right)\end{aligned} \tag{3}$$

where x_k denotes the neural activity of the k-th neuron; S_k^e and S_k^i are the excitatory and inhibitory inputs to the neuron, respectively; A is the passive decay rate; B, and D are the upper and lower bounds of the neural activity, respectively; x_l represents the neural activity of neighboring neurons to the k-th neuron; n represents the amount of neighboring neurons to the k-th neuron; $[a]^+$ is defined as $[a]^+ = \max\{a, 0\}$; $[a]^-$ is defined as $[a]^- = \max\{-a, 0\}$; and σ is the threshold of the inhibitory lateral neural connections. Several robotic navigation and control algorithms have been developed depending on the shunting model [22]. The connection weight, w_{kl} and v_{kl}, are defined as

$$w_{kl} = f(|kl|) = \begin{cases} \mu/|kl|, & 0 < |kl| \le r_0 \\ 0, & |kl| > r_0 \end{cases} \tag{4}$$

and

$$v_{kl} = \beta w_{kl}, \tag{5}$$

respectively, where β is a positive constant, $\beta \in [0, 1]$; $|kl|$ represents the Euclidean distance between the k-th neuron to the l-th neuron; μ is a positive constant. In the BINN, the excitatory signal S_k^e motivates the positive neural activity, and $\sum_{l=1}^{n} w_{kl}[x_l]^+$ term enables the positive activity to propagate the whole neural network. The inhibitory signal S_k^i motivates the negative neural activity, and $\sum_{l=1}^{n} v_{kl}[x_l - \sigma]^-$ term enables the negative activity to stay locally only in a small region because of the existence of the threshold σ. Therefore, the excitatory signal S_k^e globally influences the whole state space, while the inhibitory signal S_k^i has only a local effect in a small region, as shown in Fig. 2(b). The external input I_k varies with the generation of the force $I_k = [I_{att}, I_{rep}]$, where I_{att} and I_{rep} are external inputs when generating the attractive and repulsive forces, respectively. Based on the modeling of the fish-inspired behavior, the *Follow* robots need to track the *Escape* robot or the lowest hierarchical index *Follow* robot. The lower hierarchical index robot indicates it is closer to the *Escape* robot, which has higher probabilities of the correct moving direction to the *Escape* robot. Thus, the external input I_{att} is defined as

$$I_{att} = \begin{cases} E, & \text{if it is a } \textit{Escape} \text{ or lowest index robot} \\ -E, & \text{if it is an obstacle} \\ 0, & \text{otherwise} \end{cases} \tag{6}$$

where E is a positive constant. If the corresponding position of the neuron is the *Escape* robot or the lowest index robot, the external input becomes a large positive value. If the corresponding position is the obstacle, the external input becomes a large negative value. The command neuron of the attractive force can be given as

$$P_{att} \Leftarrow x_{P_{att}} = \max\{x_l, l = 1, 2, ..., n\} \tag{7}$$

where P_{att} represents the command neuron of the attractive force in the neural network; $x_{P_{att}}$ represents the neural activity of the command neuron of the attractive force. From (7), the robot keeps searching for maximum neural activity from its neighborhoods. When a robot advances to a new position, the new position becomes its current position. The attractive force $\overline{\mathbf{f_A}(\mathbf{k}, \mathbf{l})}$ can be defined as

$$\overline{\mathbf{f_A}(\mathbf{k}, \mathbf{l})} = C_A \frac{P_{att} - P_c}{\|P_{att} - P_c\|} \tag{8}$$

where C_A is a positive constant; P_c is the current position of the robot. The swarm robots are required to maintain the desired distance R_d to each other. Thus, the external input I_{rep} is defined as

$$I_{rep} = \begin{cases} E, & \text{if it is a neighbor robot} \\ -E, & \text{if it is an obstacle} \\ 0, & \text{otherwise.} \end{cases} \tag{9}$$

If the corresponding position of the neuron is a threat or neighbor robot, the external input becomes a large positive value. If the corresponding position is an obstacle, the

external input becomes a large negative value. The command neuron of the repulsive force can be given as

$$P_{rep} \Leftarrow x_{P_{rep}} = \min\{x_l, l = 1, 2, ..., n; x_l \geq 0\} \tag{10}$$

where P_{rep} represents the command neuron of the robot; $x_{P_{rep}}$ represents the neural activity of the command neuron of the repulsive force. The *Escape* robot has information about the threat position, thus the *Escape* robot only choose the minimum and positive neuron to generate the collision-free escape trajectory. The repulsive force of the *Follow* robot $\overline{\mathbf{f_R}(\mathbf{k},\mathbf{l})}$ can be defined as

$$\overline{\mathbf{f_R}(\mathbf{k},\mathbf{l})} == \begin{cases} C_R \frac{P_{rep} - P_c}{\|P_{rep} - P_c\|} & \text{if } 0 < D(k,l) \leq R_d \\ \overline{\mathbf{0}}, & \text{if } D(k,l) > R_d \end{cases} \tag{11}$$

where C_R is a positive constant; $D(k,l)$ is the distance between two neighboring robots k and l. The repulsive force of the *Follow* robot takes effect only if the distance of neighboring robots is smaller than R_d. The robot keeps searching for a minimum and positive neural activity from its neighborhoods.

C. Self-adaptive Collective Mechanism

During the escape process, the swarm robots are required to be self-adaptive to adapt to dynamic environments, which means the swarm robots should be able to dynamically adjust their movement parameters based on the environment. The resultant force of each robot can be given as

$$\overline{\mathbf{F_{RS}}} = \alpha_A \sum_{l \in N(I), h_l < h_k} \overline{\mathbf{f_A}(\mathbf{k},\mathbf{l})} + \alpha_R \sum_{l \in N(I)} \overline{\mathbf{f_R}(\mathbf{k},\mathbf{l})} \tag{12}$$

where α_A and α_R, $0 \leq \alpha_A, \alpha_R \leq 1$ and $\alpha_A + \alpha_R = 1$, are self-adaptive weights of the attractive and repulsive forces, respectively. The self-adaptive motion is to dynamically adjust the proper ratio of α_A / α_R to adapt to the environment. In previous studies, the ratio of α_A / α_R only depended on the average neighboring distance of robots [23]. However, in the dynamic obstacle environment, the average distance is not an accurate indicator to evaluate the ratios because the effect of obstacles is ignored when the obstacle partitions robots. In the proposed method, the dynamic neural activity is incorporated into the adjustment of the α_A / α_R ratio. The stride lengths of adjustment Δ can be defined as

$$\Delta = \begin{cases} +U, & \text{if } \mathrm{Avr(i)} + \sum_{l=1}^{n} [x_l]^- > R_d \\ -U, & \text{if } \mathrm{Avr(i)} + \sum_{l=1}^{n} [x_l]^- \leq R_d \end{cases} \tag{13}$$

where U is a small constant and function $\mathrm{Avr(i)}$ denotes the average neighboring distance of robot i. If there are no obstacles near robots, $\sum_{l=1}^{n} [x_l]^- = 0$, robots adjust the ratio based on the average neighboring distance. If there are obstacles near robots, $\sum_{l=1}^{n} [x_l]^-$ is a positive value. Thus, the attraction effect continuously increases, which ensures robots keep connected with each other to bypass obstacles.

The magnitude of $\overline{\mathbf{F_{RS}}}$ is used to determine the velocity of the robot v_k. The possible magnitude of $\overline{\mathbf{F_{RS}}}$ is from 0 to $+\infty$, whereas the v_k is a limited range from 0 to the maximum velocity V_{max}. Thus, the magnitude of $\overline{\mathbf{F_{RS}}}$ is required to map into a finite velocity. The velocity of robot v_k is given by

$$v_k = \arctan\left(\left|\overline{\mathbf{F_{RS}}}\right|\right) \times (2/\pi) \times V_{\max} \tag{14}$$

where $\arctan()$ is the trigonometric function. The above nonlinear mapping has been used for the collective motion [23]. The velocity v_k increases with the increase of the magnitude of $\overline{\mathbf{F_{RS}}}$ until the force $\overline{\mathbf{F_{RS}}}$ reaches a larger magnitude, which is less sensitive to the mapping function.

IV. Simulation Results

In this section, the proposed approach is tested in different scenarios, including static obstacles, moving obstacles, and new threat scenarios. In addition, simulation results are compared with other recent approaches to illustrate the performance of environmental adaptation and self-adaptive performance. All simulation studies are tested in MATLAB R2021a. The swarm robots are randomly distributed in the environment. The parameters of all simulations are set as follows: $A = 15$, $B = 1$, $D = 1$, $\mu = 1$, $E = 70$, $\sigma = -0.5$, $L_n = 1$, $r_0 = \sqrt{2}$, $R_d = 3$, $R_s = 8$ and $V_{max} = 1.4$. The environment is represented by a neural network, which has 70×70 neurons.

A. Collective Escape in Different Scenarios

The first simulation aims to test the proposed approach with the static obstacle. As shown in Fig. 3, there are 13 robots randomly deployed in the environment, where the position of the threat is (15,15). In the beginning, one robot detects the threat and transmission to the *Escape* mode (red color), as shown in Fig. 3(a). As the *Escape* robot moves, the individual robots detect the *Escape* robot and transmission from the *Align* mode (yellow color) to the *Follow* mode (blue color), as shown in Figs. 3(b)–(e). In this process, the individual robots can be dynamically added to the swarm without the need for explicit reorganization, as shown in Figs. 3(c) and 3(d).

In the next simulation, the moving obstacles are considered in the environment. Fig.4(a) shows the moving obstacle, which continuously moves to the right. The moving obstacle might partition the swarm robots, which requires robots to maintain a connection with each other to avoid member loss. Figs. 4(b)-(e) show the swarm robots are able to bypass the moving obstacle without member loss. A different escape trajectory is generated because the moving obstacle blocks the escape direction of the swarm robot.

In the final simulation, some new threats might suddenly appear in the environment. The mode transition is dynamic because every robot that detects the new threat can transition into the *Escape* mode. As shown in Figs. 5(a) and 5(b), robots start to escape the threat until a new Threat 2 is detected at time 25s. The robot with *Escape* mode transitions into the *Follow* mode, whereas the robot with *Follow* mode transitions into the *Escape* mode, as shown in Fig. 5(c). The new collision-free escape trajectories are generated. Note that

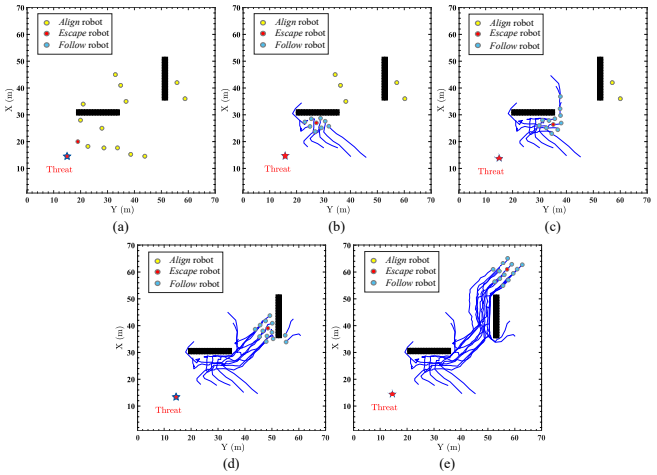

Fig. 3: Multi-robot escape in a static environment. (a) the initial position of robots; (b) escape at time $8s$; (c) escape at $16s$; (d) escape at $43s$; (e) escape at $52s$.

the influence of Threats 1 and 2 continuously exist in the neural network. Thus, the swarm robots will not return back to Threats 1 or 2 when another threat appears, as shown in Fig. 5(e).

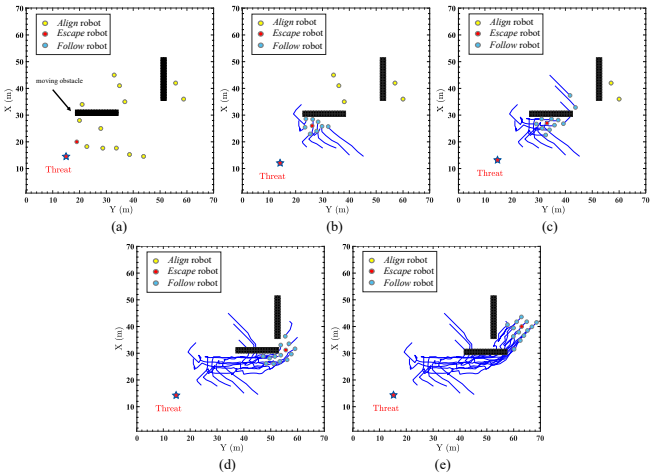

Fig. 4: Multi-robot escape in a dynamic environment. (a) the initial position of robots and moving obstacles; (b) escape at $7s$; (c) escape at $14s$; (d) at $36s$; (e) escape at $45s$.

B. Comparison Studies

To evaluate the performance of the proposed approach, a total of 30 test cases are conducted in each evaluation. In these tests, the positions of robots, threats, and obstacles are randomly distributed in the environment. The proposed approach is compared to an ablative version that lacks the self-adaptive mechanism. The self-adaptive ratio, α_A/α_R, is set to a constant without changes during the escape process. The results, shown in Fig. 6, demonstrate that the proposed approach is more effective in all scenarios, particularly in the moving obstacles scenario, where it saves over 31% of the escape time and 30% of the escape consumption. This

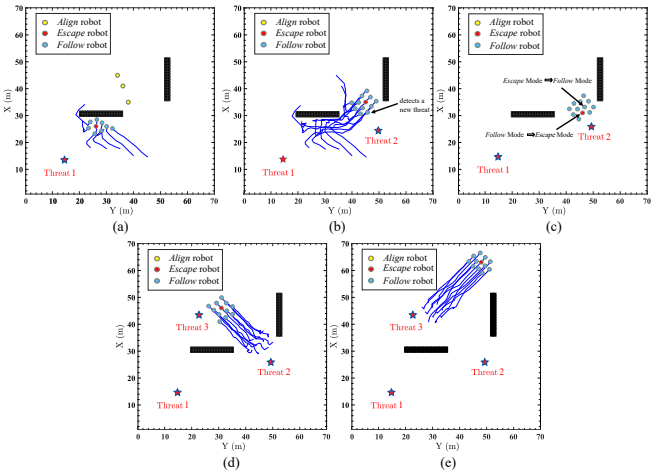

Fig. 5: Multi-robot escape in a sudden change environment. (a) escape at $6s$; (b) a new threat is detected at $25s$; (c) two robots transition their mode at $26s$; (d) a new threat is detected at $41s$; (e) escape at $61s$.

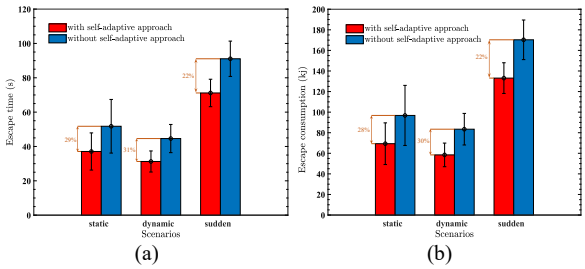

Fig. 6: Comparisons of escape time and energy consumption in different scenarios. (a) escape time; (b) energy consumption.

highlights the importance of the self-adaptive mechanism in providing effective escape solutions.

In addition, the state-of-the-art methods are compared with the proposed approach in the moving obstacles scenario, as shown in Table I. Comparing Berlinger *et al.*'s method and the proposed approach, the success rate of Berlinger *et al.*'s method is low because this approach only considers a collision-free environment and the generated escape trajectory is inefficient as it requires the robots to maintain a constant angle to the threat. Berlinger *et al.*'s method may be able to mimic fish escape behavior, but it has limitations in its practical application.

Comparing Novák *et al.*'s method and the proposed approach, Novák *et al.*'s method is limited in its ability to provide efficient escape solutions because both the threat and dynamic obstacles are considered as the same influence. On the contrary, the proposed approach uses two external inputs, S_k^e, and S_k^i. This allows the mode to provide more accurate and effective escape solutions. As shown in Table I, the success rate of the proposed approach is significantly higher than that of Novák *et al.*'s method. This is because the escape force generated by Novák *et al.*'s method may cancel each other out in multiple obstacle environment, leading to

disorientation and loss of some members within the swarm during the evasion process.

The proposed neurodynamics-based self-adaptive mechanism is compared with Zhao *et al.*'s method, which is based on the average distance of neighboring robots, in a scenario involving moving obstacles. The results, shown in Table I, indicate that the proposed approach is more efficient in terms of escape consumption and time. Note that there is a significant difference in the escape time. The proposed approach results in an escape time of $42.7s$, while Zhao *et al.*'s method results in an escape time of $62.5s$. This difference is due to the fact that Zhao *et al.*'s method involves a decrease in moving speed when robots bypass obstacles, as the support force from the obstacle cancels out the virtual force perpendicular to the obstacle. In contrast, the proposed approach relies only on dynamic neural activity for obstacle avoidance, allowing for constant moving speed during the escape process.

TABLE I: The comparison of escape performance to the state-of-the-art methods in the moving obstacles scenario

Method	Escape Consumption	Escape Time	Success Rate
Berlinger *et al.* [14]	$216.71kJ$	$87.2s$	31%
Novák *et al.* [17]	$132.12kJ$	$50.1s$	46%
Zhao *et al.* [23]	$125.62kJ$	$62.5s$	77%
Proposed approach	$116.45kJ$	$42.7s$	100%

V. Experiments

The proposed self-adaptive escape approach was tested using multiple mobile robots in a real-world environment. Three Robot Operating System (ROS) robots were built for experimental purposes. Each robot carried a 1080p camera implemented in Ubuntu using the OpenCV library and one RPLIDAR A1 laser scanner, which has $12m$ and $360°$ omnidirectional range scanning. In addition, the mobile robot contains Raspberry Pi 4 Model B and STM32F405 computing boards for robot control, environment detection, and localization. The experiment is within an area of $5m \times 3.5m$ where robot movements were recorded via a 1080p Camera. Three polyhedral and static obstacles are considered and the threat is chosen as a box with biohazard labeling.

To validate the real-world performance of the proposed approach. Three environmental scenarios are tested as shown in Fig. 7. The green lines show the escape trajectories of three mobile robots. Figs. 7(a)-(c) show the experimental results in the static environment. In particular, when robot R1 detects the threat, mobile robots R1 and R2 move under the obstacle to escape from the threat, as shown in Figs. 7(b) and 7(c). Figs. 7(d)-(f) show a dynamic environment that a moving obstacle (an orange color robot) moves to the position under the static obstacle and blocks the escape directions of mobile robots. Since mobile robots are not able to pass the obstacle through the trajectory in Figs. 7(c), new trajectories are generated as shown in Figs. 7(e) and 7(f). The dynamic response of mobile robots to changing environments can be better understood by comparing the new

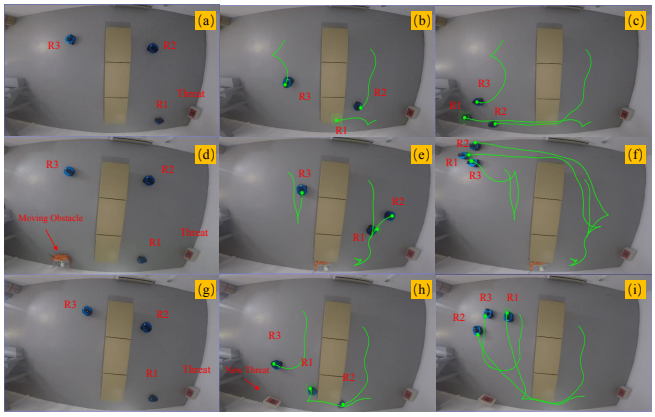

Fig. 7: Mobile robots experiments in different scenarios. (a) the initial positions of the static obstacle experiment; (b) static environment at time $5.5s$; (c) static environment at time $15.5s$; (d) the initial positions of the moving obstacle experiment; (e) dynamic environment at time $9s$; (f) dynamic environment at time $21s$; (g) the initial positions of the new threat experiment; (h) new threat environment at time $9.5s$; (i) new threat environment at time $20.5s$.

threat scenarios in Figs. 7(g)-(i). Since a new threat suddenly adds to the environment, robot R3 transitions into the *Escape* mode, and robot R1 transitions into the *Follow* mode. The new trajectory of robot R3 is to escape the threat. In real-robot experiments, each robot moves in a safe state trajectory due to the self-adaptive mechanism and the threshold of inhibitory connection σ.

VI. Conclusion

In this paper, a novel fish-inspired self-adaptive approach is proposed for the collective escape of swarm robots. The proposed approach draws inspiration from the natural observation that fish schools are capable of efficiently executing escape maneuvers with minimal communication. A novel virtual forces approach is proposed to guide swarm robots to escape the threat without collision through the dynamic landscape of neural activity. Moreover, a novel neurodynamics-based self-adaptive mechanism is proposed to improve the self-adaptive performance of swarm robots in changing environments. Several simulation and experimental results validate the escape performance of the proposed approach to facilitate safe navigation and effective self-adaptive collaboration among swarm robots that can ensure the successful execution of escape operations in variable conditions. The proposed approach may contribute to the development of biologically inspired methodologies in other fields of study and offer new insights for experimentation in animal behavior research. In future studies, the real-world experiment will increase the number of robots to validate the collective performance of the swarm robots. In addition, future research will also consider other robot types in diverse real-world settings, such as aquatic robots executing escape maneuvers in underwater environments with the presence of uncertainties such as ocean and river currents.

REFERENCES

[1] Z. Zhang, X. Zhao, B. Tao, and H. Ding, "Distributed gossip-triggered control for robot swarms with limited communication range," *IEEE Transactions on Industrial Electronics*, vol. 70, no. 12, pp. 12 511 – 12 521, 2023.

[2] D. Yu, C. P. Chen, and H. Xu, "Intelligent decision making and bionic movement control of self-organized swarm," *IEEE Transactions on Industrial Electronics*, vol. 68, no. 7, pp. 6369–6378, 2020.

[3] D. Roy, A. Chowdhury, M. Maitra, and S. Bhattacharya, "Geometric region-based swarm robotics path planning in an unknown occluded environment," *IEEE Transactions on Industrial Electronics*, vol. 68, no. 7, pp. 6053–6063, 2020.

[4] C. C. Ioannou, "Swarm intelligence in fish? the difficulty in demonstrating distributed and self-organised collective intelligence in (some) animal groups," *Behavioural processes*, vol. 141, pp. 141–151, 2017.

[5] C. Doran, D. Bierbach, J. Lukas, P. Klamser, T. Landgraf, H. Klenz, M. Habedank, L. Arias-Rodriguez, S. Krause, P. Romanczuk *et al.*, "Fish waves as emergent collective antipredator behavior," *Current Biology*, vol. 32, no. 3, pp. 708–714, 2022.

[6] C. C. Ioannou, I. D. Couzin, R. James, D. P. Croft, and J. Krause, "Social organisation and information transfer in schooling fish," *Fish cognition and behavior*, vol. 2, pp. 217–239, 2011.

[7] J. Montgomery, S. Coombs, and M. Halstead, "Biology of the mechanosensory lateral line in fishes," *Reviews in Fish Biology and Fisheries*, vol. 5, pp. 399–416, 1995.

[8] P. Duraisamy, R. Kumar Sidharthan, and M. Nagarajan Santhanakrishnan, "Design, modeling, and control of biomimetic fish robot: A review," *Journal of Bionic Engineering*, vol. 16, pp. 967–993, 2019.

[9] B. Chen and H. Jiang, "Swimming performance of a tensegrity robotic fish," *Soft robotics*, vol. 6, no. 4, pp. 520–531, 2019.

[10] Q. Zhong, J. Zhu, F. E. Fish, S. J. Kerr, A. Downs, H. Bart-Smith, and D. Quinn, "Tunable stiffness enables fast and efficient swimming in fish-like robots," *Science Robotics*, vol. 6, no. 57, p. eabe4088, 2021.

[11] S. Dai, Z. Wu, P. Zhang, M. Tan, and J. Yu, "Distributed formation control for a multi-robotic fish system with model-based event-triggered communication mechanism," *IEEE Transactions on Industrial Electronics*, 2023.

[12] Y. Ishiwaka, X. S. Zeng, M. L. Eastman, S. Kakazu, S. Gross, R. Mizutani, and M. Nakada, "Foids: bio-inspired fish simulation for generating synthetic datasets," *ACM Transactions on Graphics (TOG)*, vol. 40, no. 6, pp. 1–15, 2021.

[13] R.-D. Cioarga, M. V. Micea, V. Cretu, and V. Groza, "Evaluation of fish shoal inspired movement in collaborative robotic environments," in *2010 IEEE Instrumentation & Measurement Technology Conference Proceedings*, 2010, pp. 1539–1544.

[14] F. Berlinger, P. Wulkop, and R. Nagpal, "Self-organized evasive fountain maneuvers with a bioinspired underwater robot collective," in *IEEE International Conference on Robotics and Automation*, Xi'an, China, May. 30- Jun. 5 2021, pp. 9204–9211.

[15] F. Berlinger, M. Gauci, and R. Nagpal, "Implicit coordination for 3d underwater collective behaviors in a fish-inspired robot swarm," *Science Robotics*, vol. 6, no. 50, p. eabd8668, 2021.

[16] J. Connor, M. Joordens, and B. Champion, "Fish-inspired robotic algorithm: mimicking behaviour and communication of schooling fish," *Bioinspiration & Biomimetics*, vol. 18, no. 6, p. 066007, 2023.

[17] F. Novák, V. Walter, P. Petráček, T. Báča, and M. Saska, "Fast collective evasion in self-localized swarms of unmanned aerial vehicles," *Bioinspiration & biomimetics*, vol. 16, no. 6, p. 066025, 2021.

[18] H. Min and Z. Wang, "Design and analysis of group escape behavior for distributed autonomous mobile robots," in *IEEE International Conference on Robotics and Automation*, Shanghai, China, May 2011, pp. 6128–6135.

[19] T. Nogami and Z. Wang, "Group behavior on emergency mode transferring in autonomous multi-robot systems with subgroups," in *2019 IEEE International Conference on Robotics and Biomimetics (ROBIO)*. IEEE, 2019, pp. 654–659.

[20] M. Nagy, Z. Ákos, D. Biro, and T. Vicsek, "Hierarchical group dynamics in pigeon flocks," *Nature*, vol. 464, no. 7290, pp. 890–893, 2010.

[21] S. Grossberg, "Nonlinear neural networks: Principles, mechanisms, and architectures," *Neural Networks*, vol. 1, no. 1, pp. 17–61, 1988.

[22] J. Li, Z. Xu, D. Zhu, K. Dong, T. Yan, Z. Zeng, and S. X. Yang, "Bio-inspired intelligence with applications to robotics: a survey," *Intelligence & Robotics*, vol. 1, no. 1, pp. 58–83, 2021.

[23] H. Zhao, H. Liu, Y.-W. Leung, and X. Chu, "Self-adaptive collective motion of swarm robots," *IEEE Transactions on Automation Science and Engineering*, vol. 15, no. 4, pp. 1533–1545, 2018.